Searth for right-handed neutrino with solar neutrino experiment

Yutao Zhu, Shaomin Chen, and Zhicai Zhang*
Department of Engineering Physics, Tsinghua University, Beijing 100084, China
(Dated: August 18, 2024)

A searth for right-handed neutrino with solar neutrino experiment is presented.

I. INTRODUCTION

II. PRODUCTION AND DECAY OF RIGHT-HANDED NEUTRINO

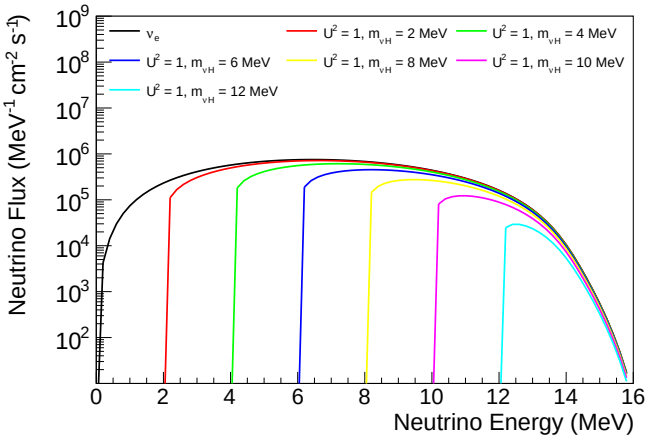

FIG. 1. Energy spectra of right-handed neutrinos with different masses emitted from ^{8}B decay in the Sun. The right-handed neutrino spectra are based on ^8B left-handed solar neutrino spectrum (ν_e in the plot, taken from [1]) and are suppressed by the mixing parameter $|U_{eH}|^2$ by $\Phi(E_{\nu H}) = |U_{eH}|^2\sqrt{1-(\frac{m_{\nu H}}{E_{\nu H}})^2}\Phi_{^8B}(E_\nu)$, where $|U_{eH}|^2$ is 1.0 in this plot.

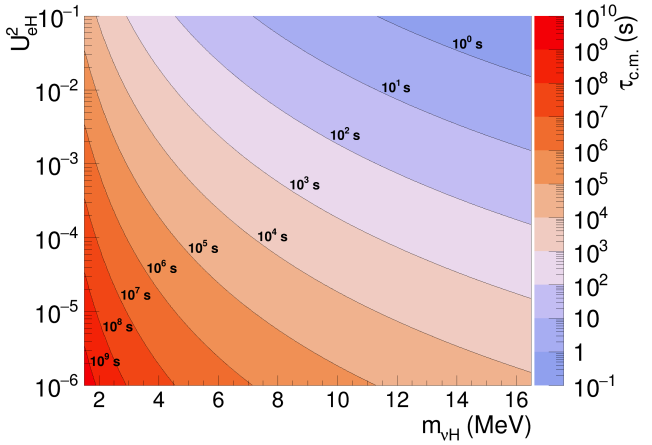

FIG. 2. Proper lifetime ($\tau_{c.m} = 1.0/\Gamma^{tot}_{c.m.}$) of right-handed neutrinos with different masses and different mixing parameter $|U_{eH}|^2$. The total width $\Gamma^{tot}_{c.m.}$ includes decays by both W and Z bosons, and is defined by $\Gamma^{tot}_{c.m.} = \frac{G_F^2}{192\pi^3}m^5_{\nu H}|U_{eH}|^2(1+h\left[\frac{m_e^2}{m^2_{\nu H}}\right])$, where $h\left[\frac{m_e^2}{m^2_{\nu H}}\right])$ is the phase-space taken from [2].

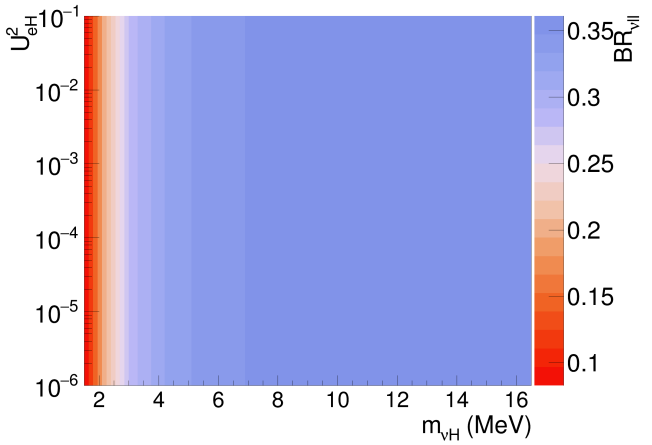

FIG. 3. Branching ratio of ν_H decay to $\nu_e e^+ e^-$ for different masses and different mixing parameter $|U_{eH}|^2$.

* zhicaizhang@tsinghua.edu.cn

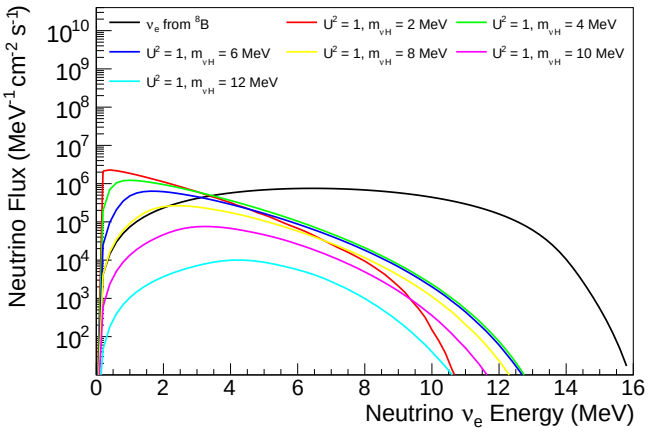

FIG. 4. Energy spectra of left-handed neutrinos (ν_e) in the lab frame from ν_H to $\nu_e e^+ e^-$ decay for different ν_H masses. The spectra shown in this plot include all ν_H decay (regardless of where they decay). The original solar neutrino energy spectrum from ^8B in the Sun is also shown in the plot (black curve).

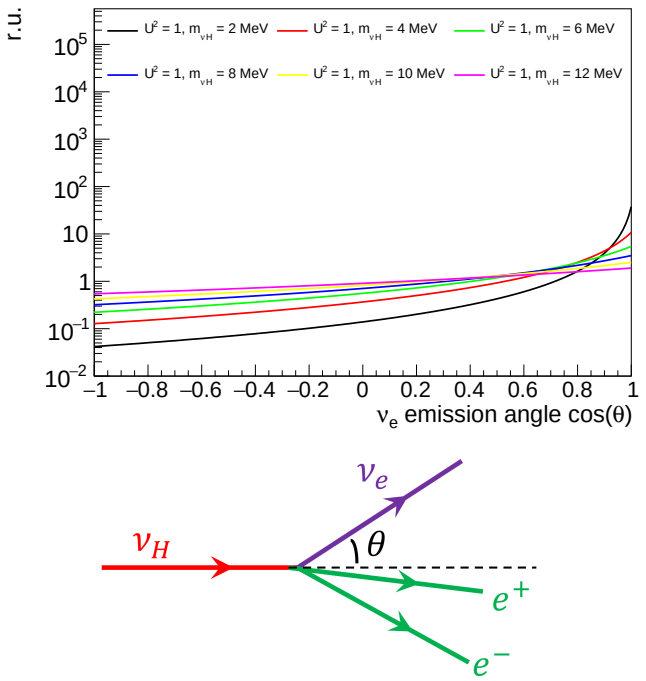

FIG. 5. Top: emission angle cos(θ) distribution of left-handed neutrinos (ν_e) in the lab frame from ν_H to $\nu_e e^+ e^-$ decay for different ν_H masses. The plots shown in this plot include all ν_H decay (regardless of where they decay). Bottom: sketch of definition of emission angle θ.

III. SEARCH FOR ν_H WITH e^+e^- SPECTRUM

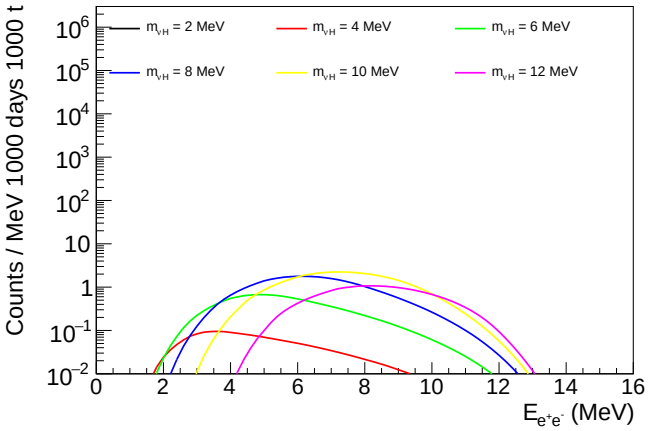

FIG. 6. The expected energy spectra of of e^+e^- pairs in the lab frame from ν_H to $\nu_e e^+e^-$ decay for different ν_H masses. The spectra only include ν_H's that decay inside a 1000-ton detector placed on earth over 1000 days. The mixing parameter $|U_{eH}|^2$ is 10^{-6} in this plot.

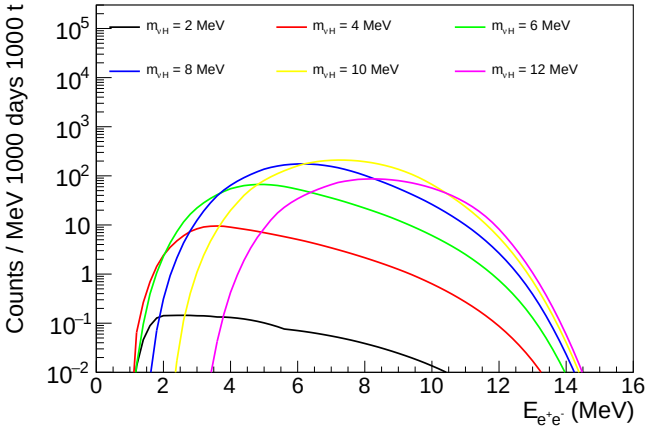

FIG. 7. The expected energy spectra of of e^+e^- pairs in the lab frame from ν_H to $\nu_e e^+e^-$ decay for different ν_H masses. The spectra only include ν_H's that decay inside a 1000-ton detector placed on earth over 1000 days. The mixing parameter $|U_{eH}|^2$ is 10^{-5} in this plot.

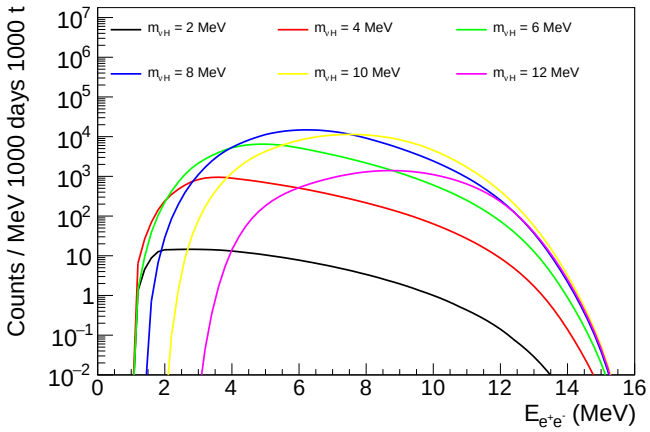

FIG. 8. The expected energy spectra of of e^+e^- pairs in the lab frame from ν_H to $\nu_e e^+e^-$ decay for different ν_H masses. The spectra only include ν_H's that decay inside a 1000-ton detector placed on earth over 1000 days. The mixing parameter $|U_{eH}|^2$ is 10^{-4} in this plot.

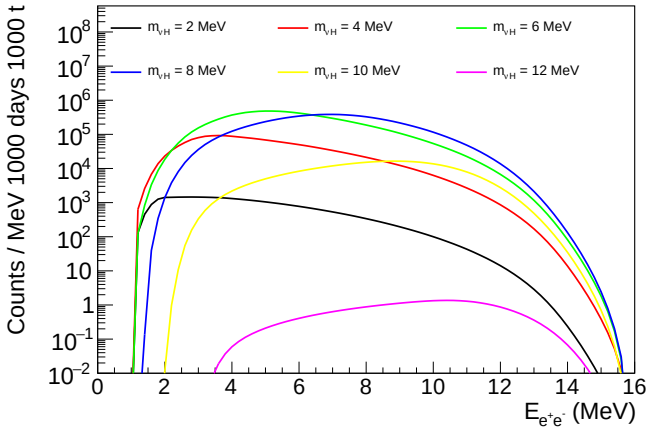

FIG. 9. The expected energy spectra of of e^+e^- pairs in the lab frame from ν_H to $\nu_e e^+e^-$ decay for different ν_H masses. The spectra only include ν_H's that decay inside a 1000-ton detector placed on earth over 1000 days. The mixing parameter $|U_{eH}|^2$ is 10^{-3} in this plot.

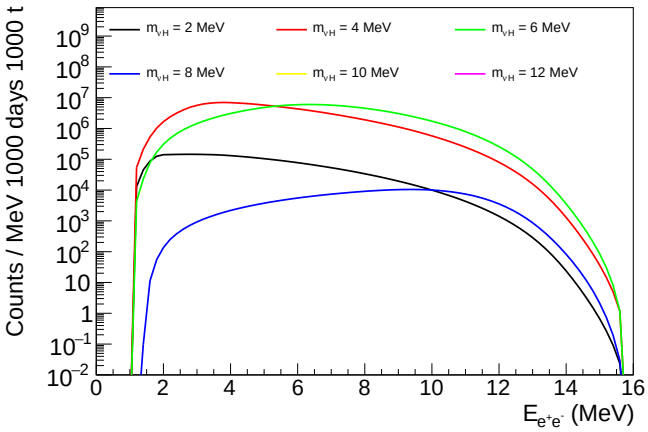

FIG. 10. The expected energy spectra of of e^+e^- pairs in the lab frame from ν_H to $\nu_e e^+e^-$ decay for different ν_H masses. The spectra only include ν_H's that decay inside a 1000-ton detector placed on earth over 1000 days. The mixing parameter $|U_{eH}|^2$ is 10^{-2} in this plot.

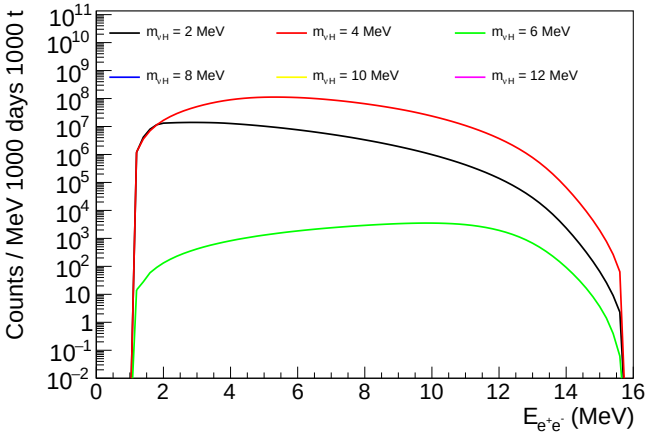

FIG. 11. The expected energy spectra of of e^+e^- pairs in the lab frame from ν_H to $\nu_e e^+e^-$ decay for different ν_H masses. The spectra only include ν_H's that decay inside a 1000-ton detector placed on earth over 1000 days. The mixing parameter $|U_{eH}|^2$ is 10^{-1} in this plot.

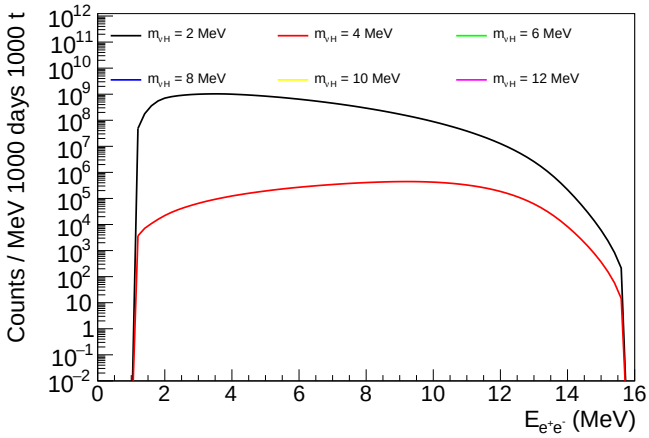

FIG. 12. The expected energy spectra of of e^+e^- pairs in the lab frame from ν_H to $\nu_e e^+e^-$ decay for different ν_H masses. The spectra only include ν_H's that decay inside a 1000-ton detector placed on earth over 1000 days. The mixing parameter $|U_{eH}|^2$ is 1.0 in this plot.

IV. SEARCH FOR ν_H WITH ν_e SOLAR ANGLE

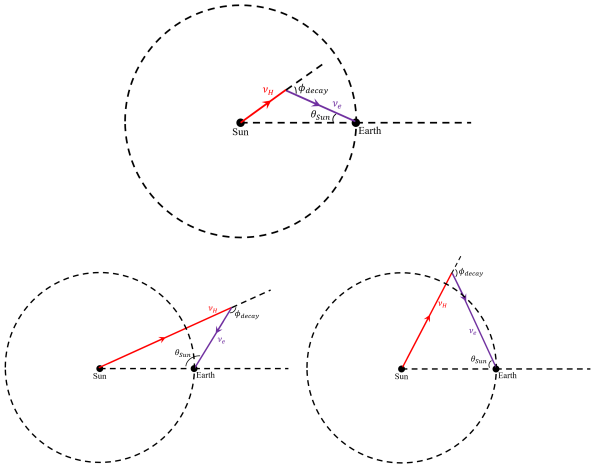

FIG. 13. Definition of angles ϕ_{decay} (emission angle) and θ_{Sun} (solar angle) for ν_H decay in flight and then the decay product ν_e reaches the detector on earth. Different scenarios of ν_H decays are shown: ν_H decay inside earth orbit (top plot), and ν_H decay outside earth orbit (bottom plots).

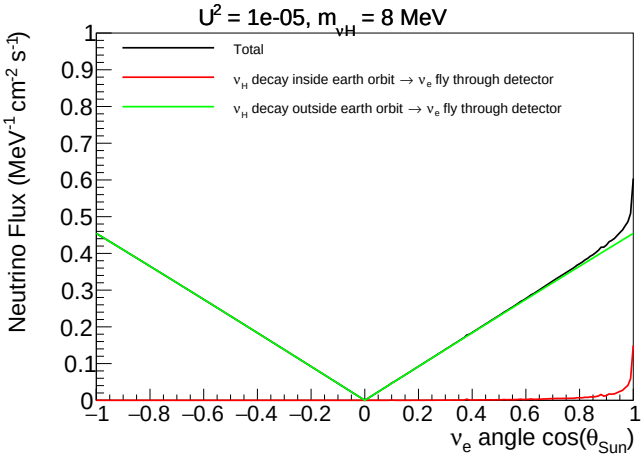

FIG. 14. Distribution solar angle $\cos(\theta_{Sun})$ of ν_e's that come from ν_H decay in flight and then reach the detector on earth. The distributions for ν_H decay inside and outside earth orbit are shown separately. The signal model shown in this plot is $m_{\nu H} = 8$ MeV and $|U_{eH}|^2 = 10^{-8}$.

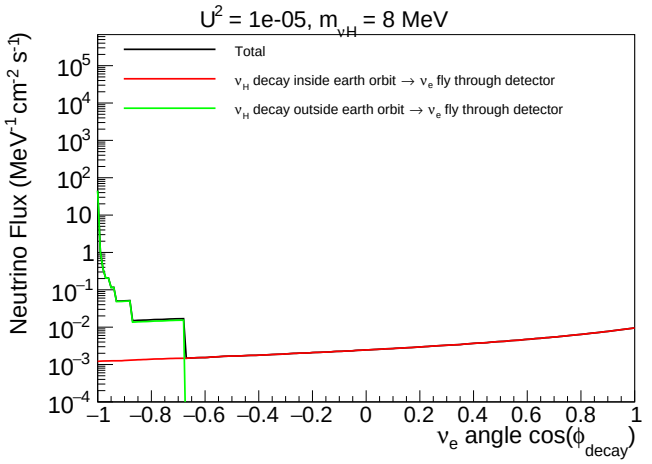

FIG. 15. Distributions of emission angle $\cos(\phi_{decay})$ of ν_e's that come from ν_H decay in flight and then reach the detector on earth. The distributions for ν_H decay inside and outside earth orbit are shown separately. The signal model shown in this plot is $m_{\nu H} = 8$ MeV and $|U_{eH}|^2 = 10^{-5}$.

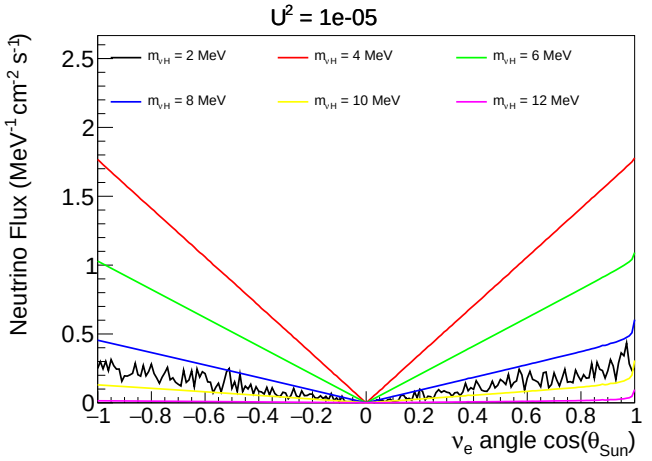

FIG. 16. Distributions of solar angle $\cos(\theta_{Sun})$ of ν_e's that come from ν_H decay in flight and then reach the detector on earth. Different curves are for different ν_H masses $m_{\nu H}$, and the mixing angle $|U_{eH}|^2 = 10^{-5}$.

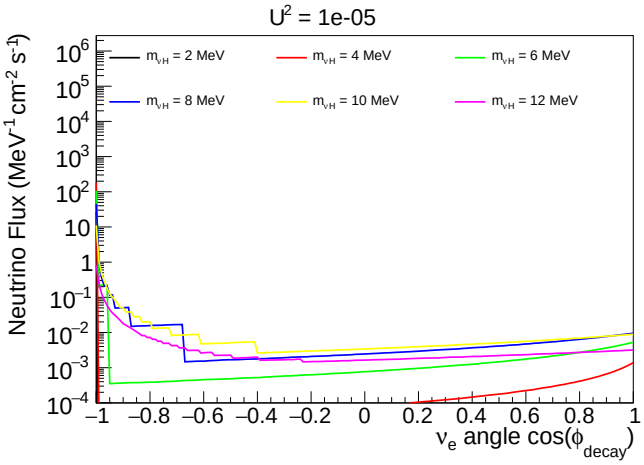

FIG. 17. Distributions of emission angle $\cos(\phi_{decay})$ of ν_e's that come from ν_H decay in flight and then reach the detector on earth. Different curves are for different ν_H masses $m_{\nu H}$, and the mixing angle $|U_{eH}|^2 = 10^{-5}$.

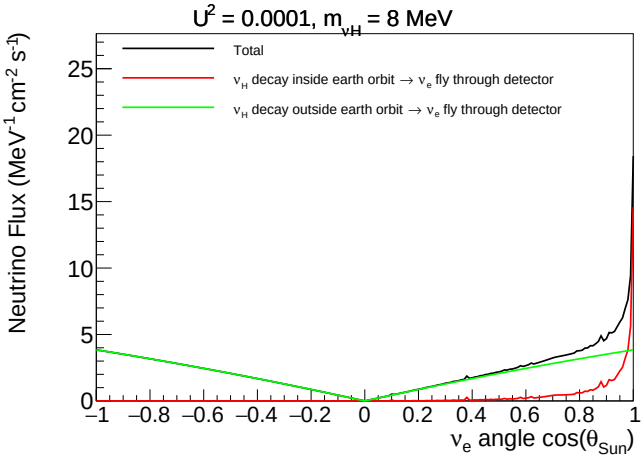

FIG. 18. Distribution solar angle $\cos(\theta_{Sun})$ of ν_e's that come from ν_H decay in flight and then reach the detector on earth. The distributions for ν_H decay inside and outside earth orbit are shown separately. The signal model shown in this plot is $m_{\nu H} = 8$ MeV and $|U_{eH}|^2 = 10^{-4}$.

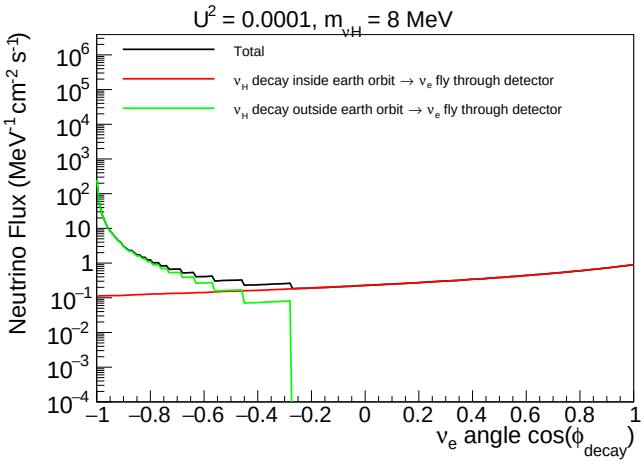

FIG. 19. Distributions of emission angle $\cos(\phi_{decay})$ of ν_e's that come from ν_H decay in flight and then reach the detector on earth. The distributions for ν_H decay inside and outside earth orbit are shown separately. The signal model shown in this plot is $m_{\nu H} = 8$ MeV and $|U_{eH}|^2 = 10^{-4}$.

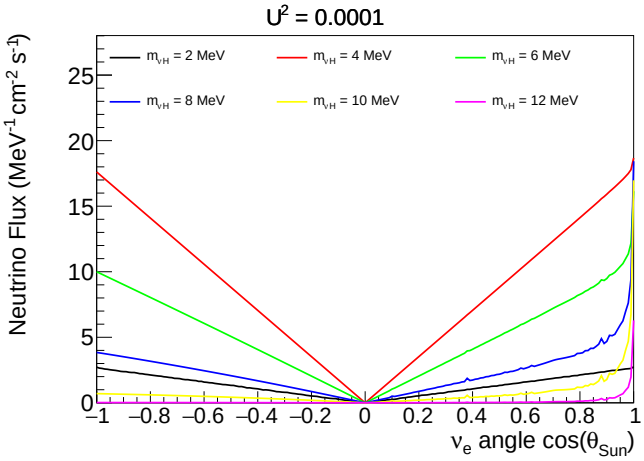

FIG. 20. Distributions of solar angle $\cos(\theta_{Sun})$ of ν_e's that come from ν_H decay in flight and then reach the detector on earth. Different curves are for different ν_H masses $m_{\nu H}$, and the mixing angle $|U_{eH}|^2 = 10^{-4}$.

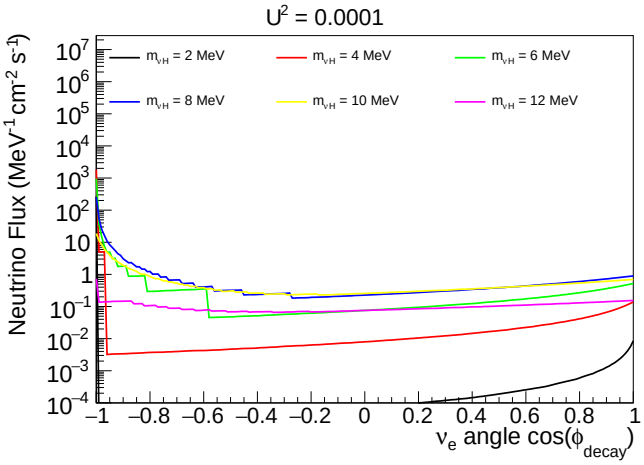

FIG. 21. Distributions of emission angle $\cos(\phi_{decay})$ of ν_e's that come from ν_H decay in flight and then reach the detector on earth. Different curves are for different ν_H masses $m_{\nu H}$, and the mixing angle $|U_{eH}|^2 = 10^{-4}$.

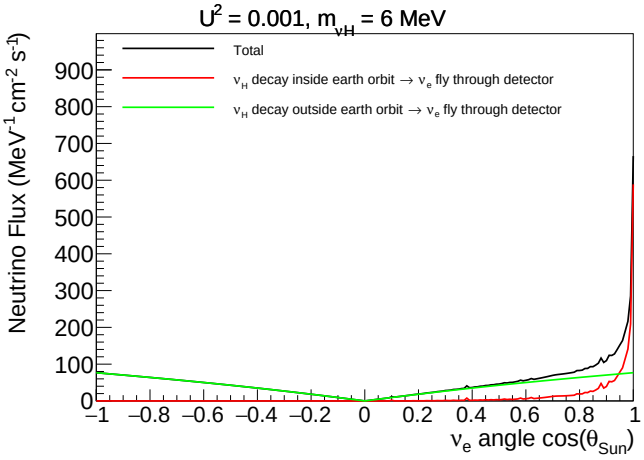

FIG. 22. Distribution solar angle $\cos(\theta_{Sun})$ of ν_e's that come from ν_H decay in flight and then reach the detector on earth. The distributions for ν_H decay inside and outside earth orbit are shown separately. The signal model shown in this plot is $m_{\nu H} = 6$ MeV and $|U_{eH}|^2 = 10^{-3}$.

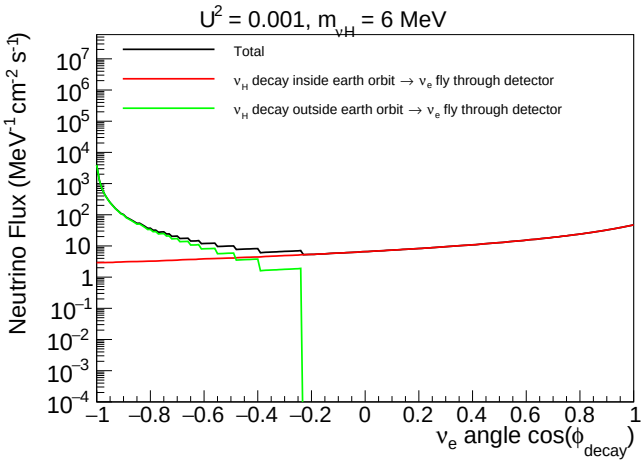

FIG. 23. Distributions of emission angle $\cos(\phi_{decay})$ of ν_e's that come from ν_H decay in flight and then reach the detector on earth. The distributions for ν_H decay inside and outside earth orbit are shown separately. The signal model shown in this plot is $m_{\nu H} = 6$ MeV and $|U_{eH}|^2 = 10^{-3}$.

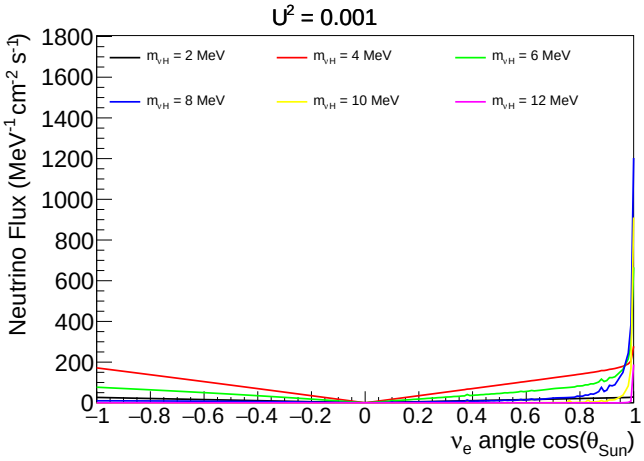

FIG. 24. Distributions of solar angle $\cos(\theta_{Sun})$ of ν_e's that come from ν_H decay in flight and then reach the detector on earth. Different curves are for different ν_H masses $m_{\nu H}$, and the mixing angle $|U_{eH}|^2 = 10^{-3}$.

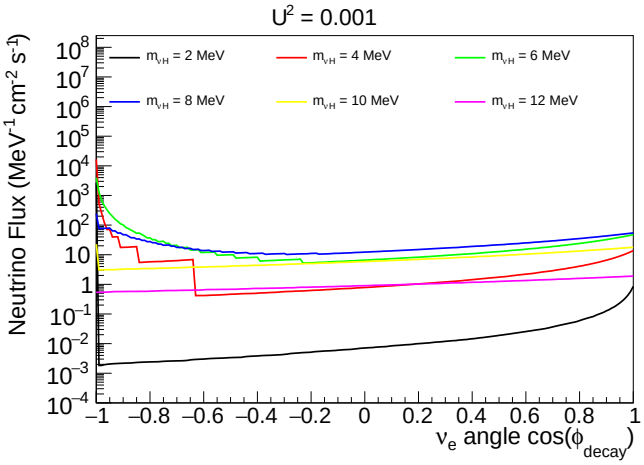

FIG. 25. Distributions of emission angle $\cos(\phi_{decay})$ of ν_e's that come from ν_H decay in flight and then reach the detector on earth. Different curves are for different ν_H masses $m_{\nu H}$, and the mixing angle $|U_{eH}|^2 = 10^{-3}$.

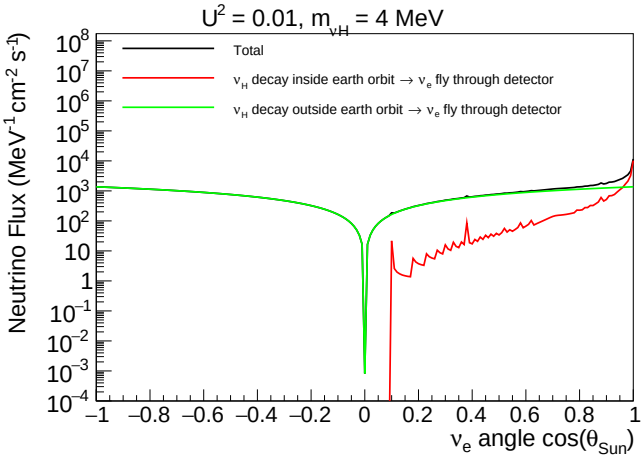

FIG. 26. Distribution solar angle $\cos(\theta_{Sun})$ of ν_e's that come from ν_H decay in flight and then reach the detector on earth. The distributions for ν_H decay inside and outside earth orbit are shown separately. The signal model shown in this plot is $m_{\nu H} = 4$ MeV and $|U_{eH}|^2 = 10^{-2}$.

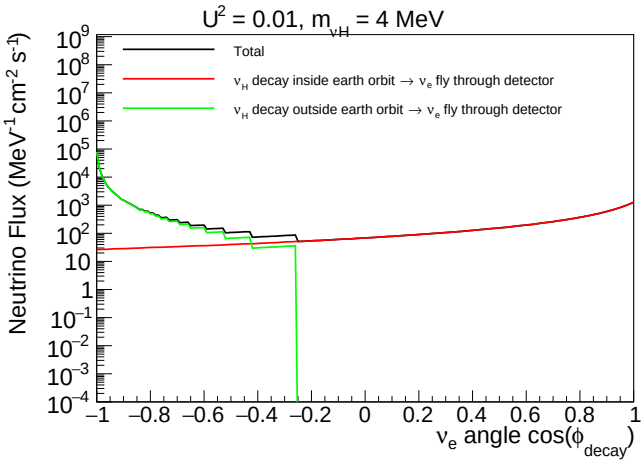

FIG. 27. Distributions of emission angle $\cos(\phi_{decay})$ of ν_e's that come from ν_H decay in flight and then reach the detector on earth. The distributions for ν_H decay inside and outside earth orbit are shown separately. The signal model shown in this plot is $m_{\nu H} = 4$ MeV and $|U_{eH}|^2 = 10^{-2}$.

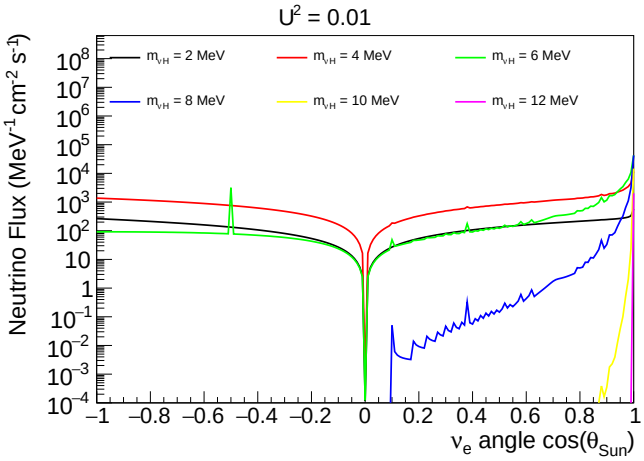

FIG. 28. Distributions of solar angle $\cos(\theta_{Sun})$ of ν_e's that come from ν_H decay in flight and then reach the detector on earth. Different curves are for different ν_H masses $m_{\nu H}$, and the mixing angle $|U_{eH}|^2 = 10^{-2}$.

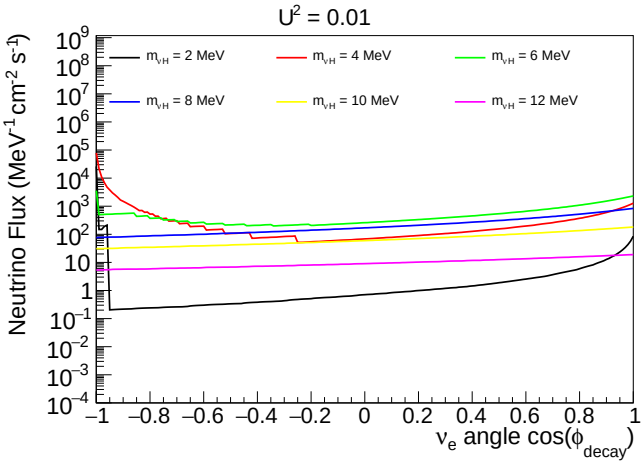

FIG. 29. Distributions of emission angle $\cos(\phi_{decay})$ of ν_e's that come from ν_H decay in flight and then reach the detector on earth. Different curves are for different ν_H masses $m_{\nu H}$, and the mixing angle $|U_{eH}|^2 = 10^{-2}$.

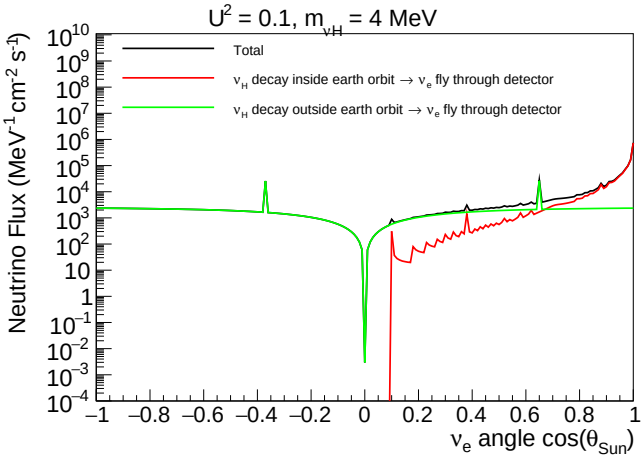

FIG. 30. Distribution solar angle $\cos(\theta_{Sun})$ of ν_e's that come from ν_H decay in flight and then reach the detector on earth. The distributions for ν_H decay inside and outside earth orbit are shown separately. The signal model shown in this plot is $m_{\nu H} = 4$ MeV and $|U_{eH}|^2 = 10^{-1}$.

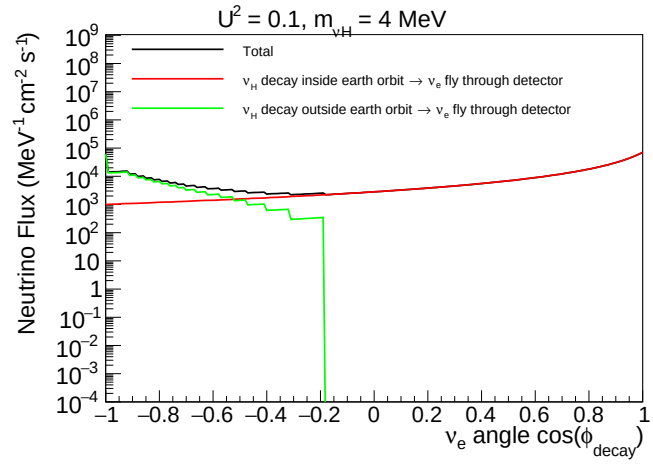

FIG. 31. Distributions of emission angle $\cos(\phi_{decay})$ of ν_e's that come from ν_H decay in flight and then reach the detector on earth. The distributions for ν_H decay inside and outside earth orbit are shown separately. The signal model shown in this plot is $m_{\nu H} = 4$ MeV and $|U_{eH}|^2 = 10^{-1}$.

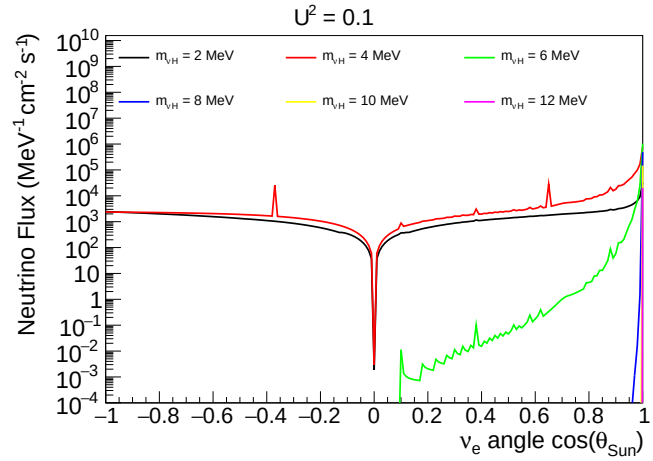

FIG. 32. Distributions of solar angle $\cos(\theta_{Sun})$ of ν_e's that come from ν_H decay in flight and then reach the detector on earth. Different curves are for different ν_H masses $m_{\nu H}$, and the mixing angle $|U_{eH}|^2 = 10^{-1}$.

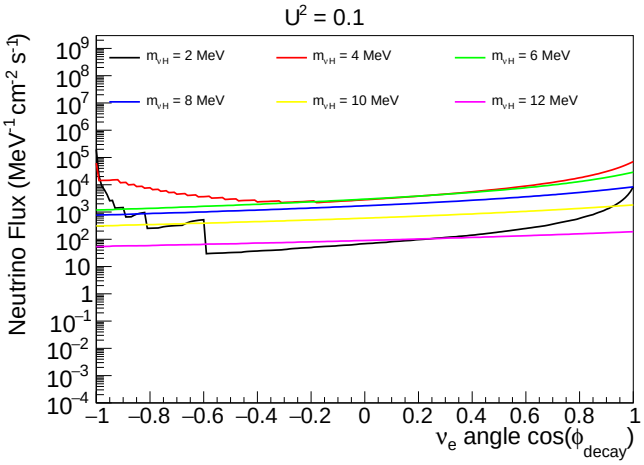

FIG. 33. Distributions of emission angle $\cos(\phi_{decay})$ of ν_e's that come from ν_H decay in flight and then reach the detector on earth. Different curves are for different ν_H masses $m_{\nu H}$, and the mixing angle $|U_{eH}|^2 = 10^{-1}$.

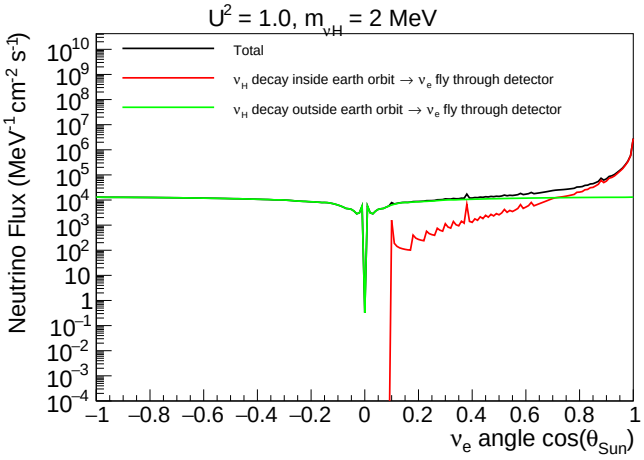

FIG. 34. Distribution solar angle $\cos(\theta_{Sun})$ of ν_e's that come from ν_H decay in flight and then reach the detector on earth. The distributions for ν_H decay inside and outside earth orbit are shown separately. The signal model shown in this plot is $m_{\nu H} = 2$ MeV and $|U_{eH}|^2 = 1.0$.

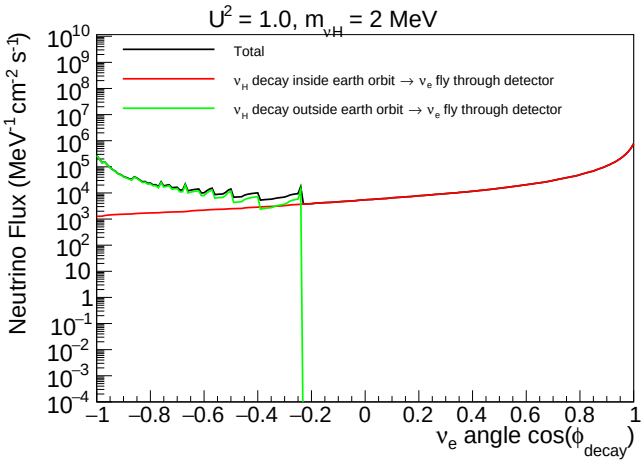

FIG. 35. Distributions of emission angle $\cos(\phi_{decay})$ of ν_e's that come from ν_H decay in flight and then reach the detector on earth. The distributions for ν_H decay inside and outside earth orbit are shown separately. The signal model shown in this plot is $m_{\nu H} = 2$ MeV and $|U_{eH}|^2 = 1.0$.

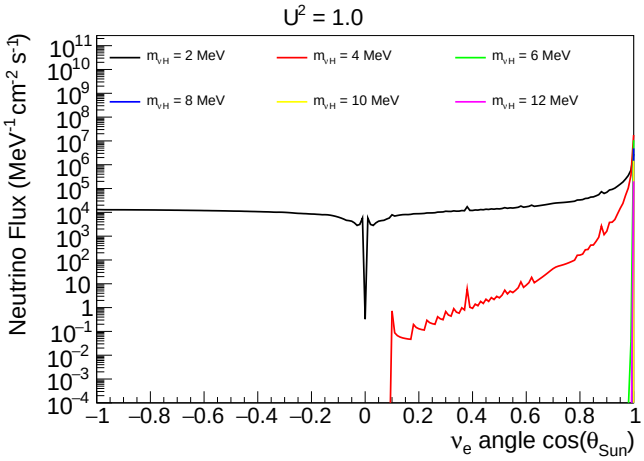

FIG. 36. Distributions of solar angle $\cos(\theta_{Sun})$ of ν_e's that come from ν_H decay in flight and then reach the detector on earth. Different curves are for different ν_H masses $m_{\nu H}$, and the mixing angle $|U_{eH}|^2 = 1$.

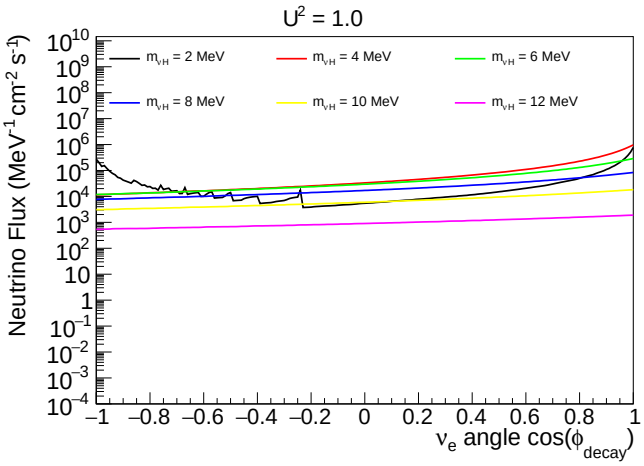

FIG. 37. Distributions of emission angle $\cos(\phi_{decay})$ of ν_e's that come from ν_H decay in flight and then reach the detector on earth. Different curves are for different ν_H masses $m_{\nu H}$, and the mixing angle $|U_{eH}|^2 = 1$.

V. SEARCH FOR ν_H WITH ν_e SPECTRUM

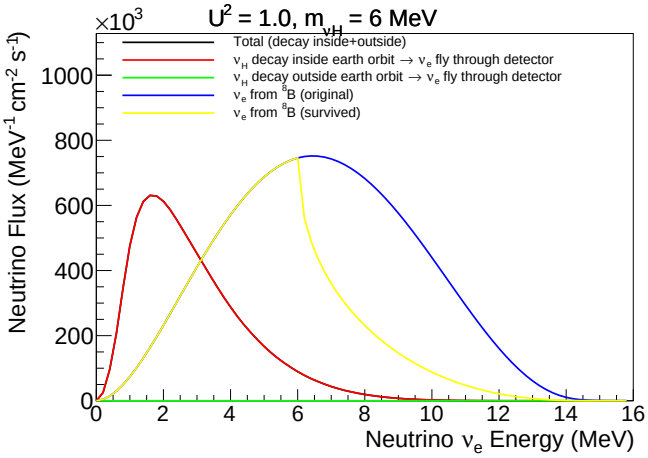

FIG. 38. Energy spectra of ν_e's that come from ν_H decay in flight and then reach the detector on earth. The spectra for ν_H decay inside and outside earth orbit are shown separately. The original solar neutrino spectrum that come from ^8B decay in the Sun, and spectrum of solar neutrino that survived the mix to ν_H during ^8B decay, are also shown in the plot. The signal model shown in this plot is $m_{\nu H} = 6$ MeV and $|U_{eH}|^2 = 1.0$.

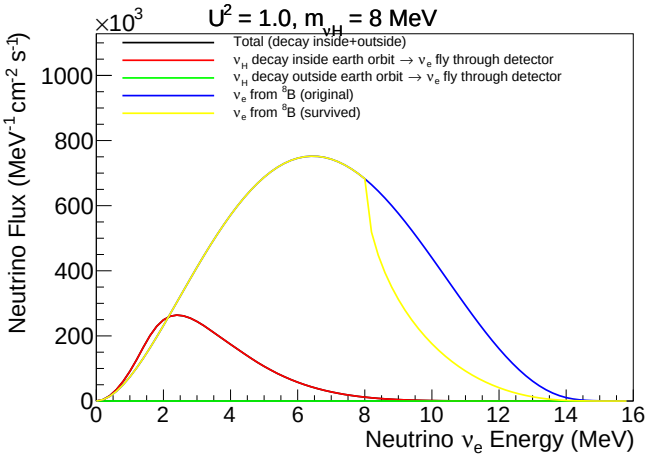

FIG. 39. Energy spectra of ν_e's that come from ν_H decay in flight and then reach the detector on earth. The spectra for ν_H decay inside and outside earth orbit are shown separately. The original solar neutrino spectrum that come from ^8B decay in the Sun, and spectrum of solar neutrino that survived the mix to ν_H during ^8B decay, are also shown in the plot. The signal model shown in this plot is $m_{\nu H} = 8$ MeV and $|U_{eH}|^2 = 1.0$.

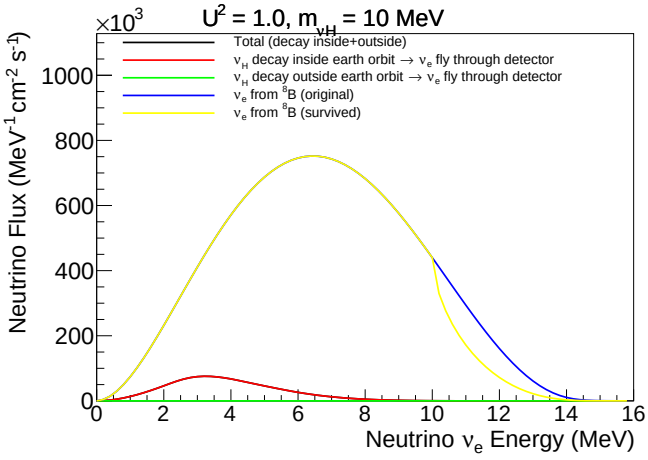

FIG. 40. Energy spectra of ν_e's that come from ν_H decay in flight and then reach the detector on earth. The spectra for ν_H decay inside and outside earth orbit are shown separately. The original solar neutrino spectrum that come from ^8B decay in the Sun, and spectrum of solar neutrino that survived the mix to ν_H during ^8B decay, are also shown in the plot. The signal model shown in this plot is $m_{\nu H} = 10$ MeV and $|U_{eH}|^2 = 1.0$.

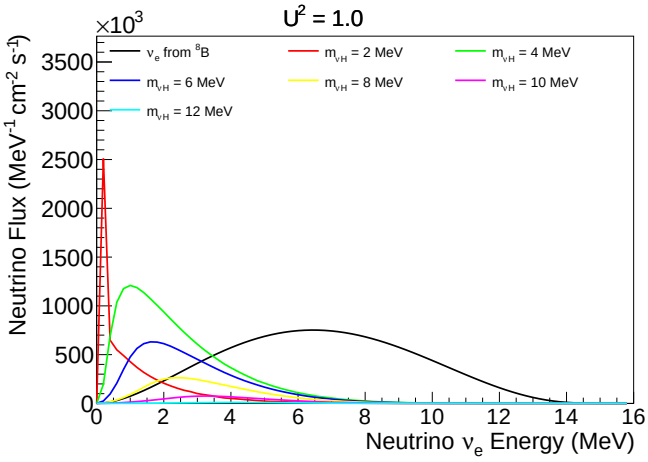

FIG. 41. Energy spectra of ν_e's that come from ν_H decay in flight and then reach the detector on earth. Different curves are for different ν_H masses $m_{\nu H}$, and the mixing angle $|U_{eH}|^2 = 1.0$. The background (original solar neutrino spectrum that come from ^8B decay in the Sun) spectrum is also shown in the plot.

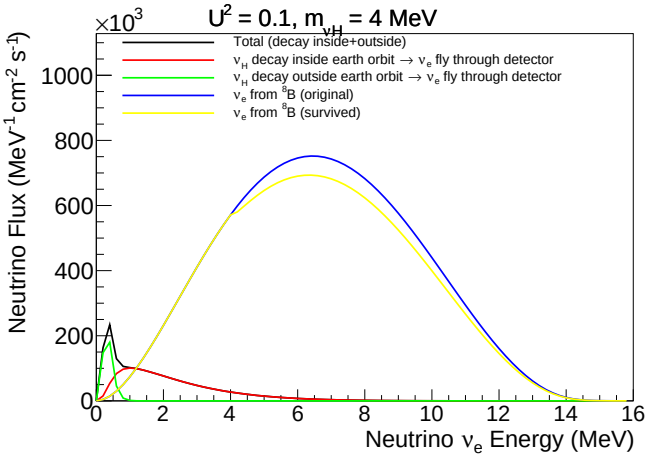

FIG. 42. Energy spectra of ν_e's that come from ν_H decay in flight and then reach the detector on earth. The spectra for ν_H decay inside and outside earth orbit are shown separately. The original solar neutrino spectrum that come from ^8B decay in the Sun, and spectrum of solar neutrino that survived the mix to ν_H during ^8B decay, are also shown in the plot. The signal model shown in this plot is $m_{\nu H} = 4$ MeV and $|U_{eH}|^2 = 10^{-1}$.

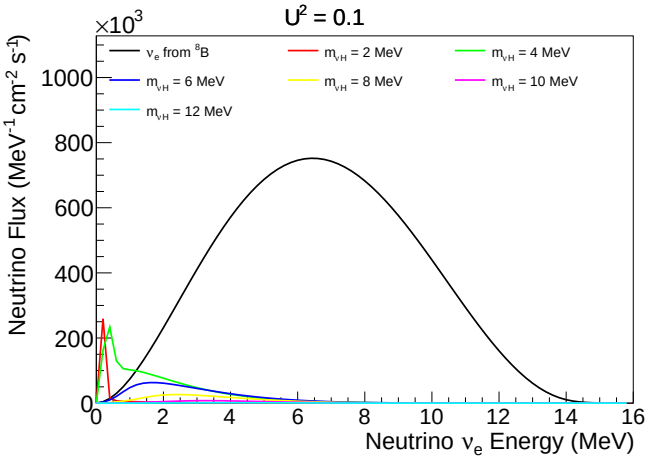

FIG. 43. Energy spectra of ν_e's that come from ν_H decay in flight and then reach the detector on earth. Different curves are for different ν_H masses $m_{\nu H}$, and the mixing angle $|U_{eH}|^2 = 10^{-1}$. The background (original solar neutrino spectrum that come from ^8B decay in the Sun) spectrum is also shown in the plot.

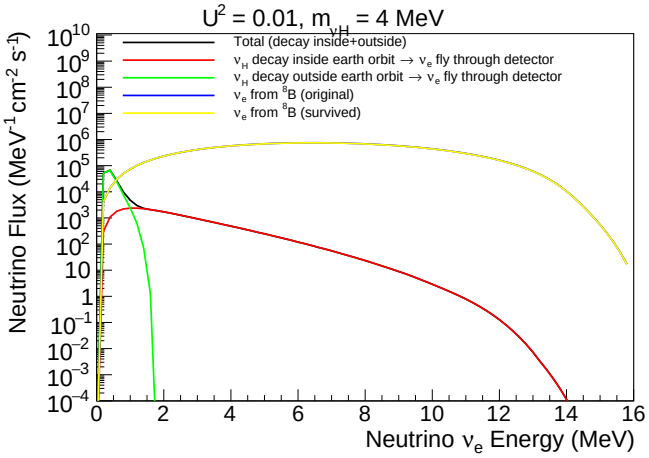

FIG. 44. Energy spectra of ν_e's that come from ν_H decay in flight and then reach the detector on earth. The spectra for ν_H decay inside and outside earth orbit are shown separately. The original solar neutrino spectrum that come from ^8B decay in the Sun, and spectrum of solar neutrino that survived the mix to ν_H during ^8B decay, are also shown in the plot. The signal model shown in this plot is $m_{\nu H} = 4$ MeV and $|U_{eH}|^2 = 10^{-2}$.

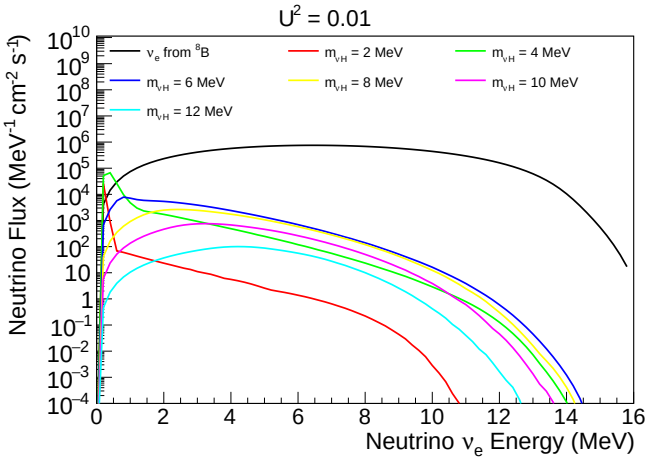

FIG. 45. Energy spectra of ν_e's that come from ν_H decay in flight and then reach the detector on earth. Different curves are for different ν_H masses $m_{\nu H}$, and the mixing angle $|U_{eH}|^2 = 10^{-2}$. The background (original solar neutrino spectrum that come from ^8B decay in the Sun) spectrum is also shown in the plot.

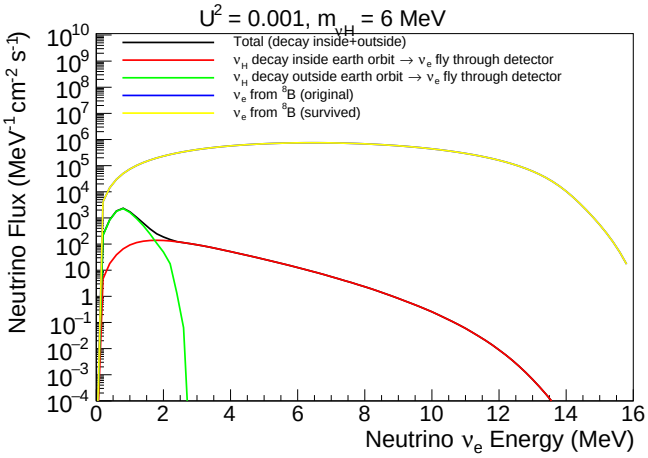

FIG. 46. Energy spectra of ν_e's that come from ν_H decay in flight and then reach the detector on earth. The spectra for ν_H decay inside and outside earth orbit are shown separately. The original solar neutrino spectrum that come from ^8B decay in the Sun, and spectrum of solar neutrino that survived the mix to ν_H during ^8B decay, are also shown in the plot. The signal model shown in this plot is $m_{\nu H} = 6$ MeV and $|U_{eH}|^2 = 10^{-3}$.

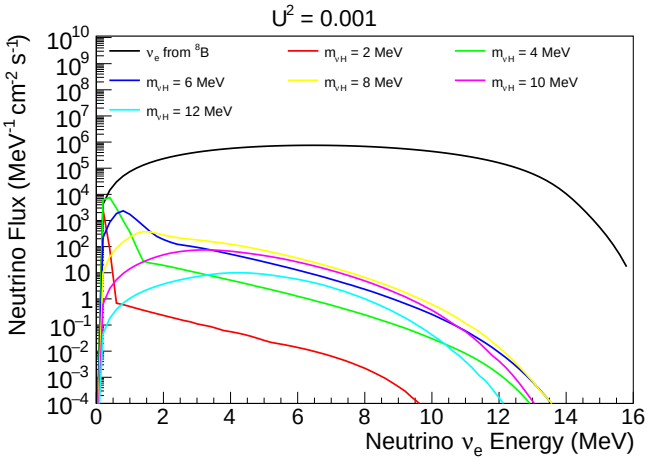

FIG. 47. Energy spectra of ν_e's that come from ν_H decay in flight and then reach the detector on earth. Different curves are for different ν_H masses $m_{\nu H}$, and the mixing angle $|U_{eH}|^2 = 10^{-3}$. The background (original solar neutrino spectrum that come from ^8B decay in the Sun) spectrum is also shown in the plot.

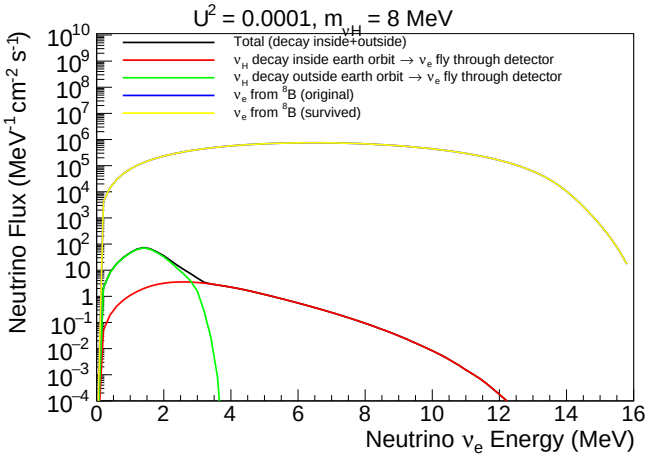

FIG. 48. Energy spectra of ν_e's that come from ν_H decay in flight and then reach the detector on earth. The spectra for ν_H decay inside and outside earth orbit are shown separately. The original solar neutrino spectrum that come from ^8B decay in the Sun, and spectrum of solar neutrino that survived the mix to ν_H during ^8B decay, are also shown in the plot. The signal model shown in this plot is $m_{\nu H} = 8$ MeV and $|U_{eH}|^2 = 10^{-4}$.

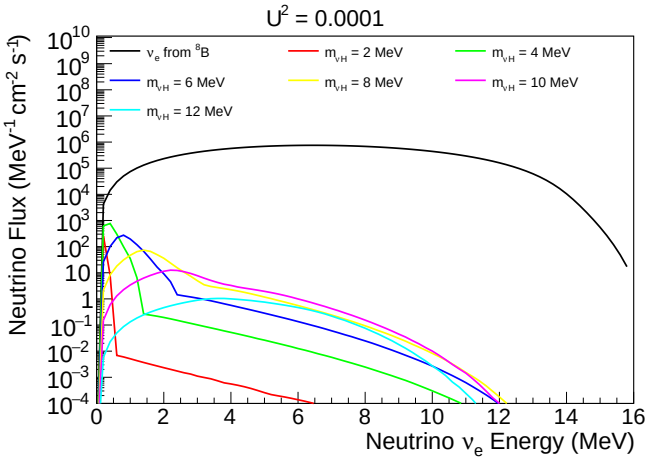

FIG. 49. Energy spectra of ν_e's that come from ν_H decay in flight and then reach the detector on earth. Different curves are for different ν_H masses $m_{\nu H}$, and the mixing angle $|U_{eH}|^2 = 10^{-4}$. The background (original solar neutrino spectrum that come from ^8B decay in the Sun) spectrum is also shown in the plot.

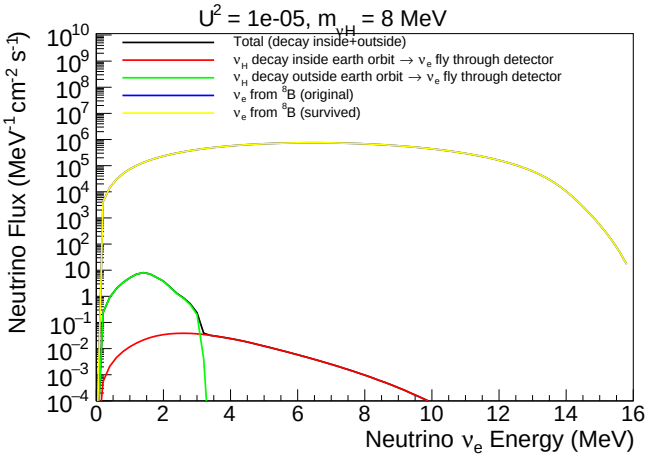

FIG. 50. Energy spectra of ν_e's that come from ν_H decay in flight and then reach the detector on earth. The spectra for ν_H decay inside and outside earth orbit are shown separately. The original solar neutrino spectrum that come from ^8B decay in the Sun, and spectrum of solar neutrino that survived the mix to ν_H during ^8B decay, are also shown in the plot. The signal model shown in this plot is $m_{\nu H} = 8$ MeV and $|U_{eH}|^2 = 10^{-5}$.

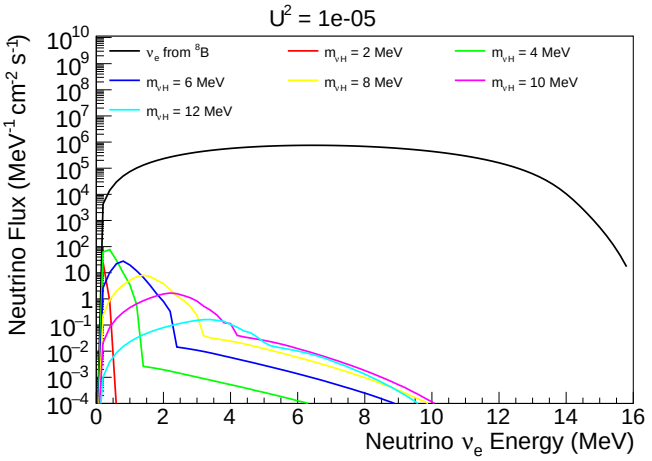

FIG. 51. Energy spectra of ν_e's that come from ν_H decay in flight and then reach the detector on earth. Different curves are for different ν_H masses $m_{\nu H}$, and the mixing angle $|U_{eH}|^2 = 10^{-5}$. The background (original solar neutrino spectrum that come from ^8B decay in the Sun) spectrum is also shown in the plot.

[1] J. N. Bahcall, E. Lisi, D. Alburger, L. De Braeckeleer, S. Freedman, and J. Napolitano, Physical Review C **54**, 411 (1996).

[2] D. Gorbunov and M. Shaposhnikov, Journal of High Energy Physics **2007**, 015 (2007).